Fachtagung "Lasermethoden in der Strömungsmesstechnik"
3. – 5. September 2013, München

Laser induzierte Fluoreszenz von Stickstoffmonoxid A-X(0,0) in einem Hochenthalpie Freistrahl

Laser Induced Fluorescence of Nitric Oxide A-X(0,0) in High Enthalpy Flow

Marco Kirschner[1], Tobias Sander[1] and Christian Mundt[1]
[1] Institute for Thermodynamics, University of the federal armed forces Munich,
85577 Neubiberg, Germany

NO-LIF, Hochenthalpie, Plasmawindkanal, Rotationstemperatur, Stickstoffmonoxid
NO-LIF, high enthalpy, plasma wind tunnel, rotational temperature, nitric oxide

Abstract

Laser induced fluorescence using the A-X(0,0) band for excitation is a promising approach to examine high enthalpy flow. Spectroscopic investigations within this excitation wavelength band intend to identify appropriate transitions that maximize fluorescence signal and minimize possible interference with other species. The feasibility of the measurement method is shown with the help of a test cell. The present work shows first qualitative measurement results of nitric oxide within a high enthalpy flow.

Introduction

Ground based facilities offer the only practical means for investigation of high enthalpy real gas effects and the simulation of flow properties that prevail during re-entry of vehicles flying through the earth's atmosphere or other planet's atmosphere. An arc heated plasma wind tunnel (total enthalpy up to 20 MJ/kg) is available at the Institute for Thermodynamics at the University of the Federal armed forces in Munich [Langkau 1981].
The characterization of the flow field is usually done by conventional diagnostic methods (thermocouple, pitot-static probes, and gas extraction). However an arcjet flow presents a challenging environment for conducting measurements as the flow is high enthalpy and chemically reacting. Therefore non-intrusive measurements are desired. Besides pointwise techniques, which imply a high measurement effort, integrative measurement methods like Schlieren, emission spectroscopy and interferometry offer a two-dimensional view, but do not allow a tomographic image. Non-intrusive laser based techniques such as Raman spectroscopy (Hatzl et al. 2011) and laser-induced fluorescence (LIF) are promising methods, in which LIF offers the great advantage of a high signal to noise ratio. In context of a plasma wind tunnel, LIF provides qualitative and quantitative flow field visualization, hence numerical simulations and radiation models can be verified and validated. An ideal tracer molecule for laser induced fluorescence measurements in high enthalpy flow is N_2, O_2 or NO. One species in high temperature air is NO, which is formed by reaction of atomic oxygen and molecular nitrogen in the air (Zeldovich-mechanism). Despite the higher partial pressure of O_2, the signal strength of NO is thought to be strong enough which is mainly influenced due to the lower cross section of O_2. Regarding the NO γ-band ($A^2\Sigma - X^2\Pi_{1/2}$) predissociative effects can be neglected, and collisional quenching is not a dominant problem in an arcjet environment (Yamada et al. 2002). As shown in Fig. 1 the A-X system and other important electronic transitions of the NO molecule are indicated on the potential energy curves.
The object of this work is the application of NO LIF to prove the technical feasibility of the measurement system, built at the plasma wind tunnel. After carrying out preliminary NO spectroscopy measurements by using an electrically heated test cell, additional measure-

ments in a high enthalpy flow will be conducted. The analysis of high resolution vibration-rotation spectra will help to identify appropriate transitions and to optimize signal strength. The selection of appropriate transitions depends on the diagnostic situation and the literature provides no clear guidelines.
As fluorescence is influenced by several collisional processes amongst others, the spectral distribution is changed by rotational energy transfer (RET) in the excited state. Moreover, interferences by other species have to be considered, for instance, a main contributor to LIF interferences is hot O_2 (Bessler et al. 2003).
Based on the aforementioned analysis, the rotational temperature of nitric oxide can be calculated using the fluorescence signal arising from excitation from different lower energy levels. One would obtain this information by executing an excitation scan. The multi-line technique offers the advantage of indicating a systematic error, if the fluorescence signals deviate from a straight line in a Boltzmann-plot and if Boltzmann distribution is assumed. This paper presents some preliminary results of the multi-line technique and visualization of nitric oxide in an arc heated wind tunnel.

Theoretical Background

The theory of LIF is well developed and reliable models are available describing transitions between different energy levels and energy transfer mechanism. In contrast to the classical mechanics, where energy varies continuously, molecules have discrete energy levels. The molecular orbital theory is necessary to predict physical and chemical properties like energy levels and electronic spectra. To understand the theoretical aspects of optically-allowed transitions in a molecule, one has to know the various spectroscopic notations. The next chapter will introduce a two-level model as well as an equation describing the fluorescence signal and the temperature dependence.

For a better understanding of the NO molecule the electron configuration and the linear combination of atomic orbitals (LCAO) is used. In case of the NO molecule only the valence orbitals are used to construct molecule orbitals (MO) sorted in ascending order with respect to the energy. To indicate which orbital (1s, 2s, 2p, …) is involved, they are usually added after the quantum number of the orbital angular moment λ. The superscript indicates the number of electrons present in the particular orbital. The NO molecule is a heteronuclear two atomic molecule, hence there is no inversion symmetry and classifying the orbitals with u and g is not required (Hollas 1995). The antibonding molecule is signed with an asterisk, thus one can write for the NO-molecule:

$$K\left(\sigma 2s\right)^2\left(\sigma^* 2s\right)^2\left(\sigma 2p\right)^2\left(\pi^* 2p\right)^4\left(\pi^* 2p\right)^1$$

Due to interaction of the orbital angular moment, spin and the electro static force between the two atomic nucleus, same configurations can comprise several energy levels. Conversely, an energy level is said to be degenerated, if a system has different quantum states at one particular energy level.

Analogous to the atomic case with Λ = 0, 1, 2, 3 the total electronic orbital angular momentum quantum number is termed Σ, Π, Δ, Φ. Further description is the notation of the various energy levels, starting with X as ground level and A, B, C etc. for higher levels. The coupling of the electron orbital angular momentum and spin is accounted for by the quantum number Ω = Σ + Λ, which is indicated by a succeeding subscript. Using the equation for multiplicity, each state is split into 2S+1 components, where S is the total spin angular moment (Herzberg 1950). Taking into account of all quantum mechanical effects and conventions given above, the appropriate term symbol for each electronic state can be written as:

$$^{2S+1}\Lambda_{\Lambda+\Sigma}$$

In quantum mechanics the energy of motion of a diatomic molecule can be considered as a simple model of mass M_1 and M_2 connected by a spring and in addition to the electronic motion, there is vibrational and rotational motion. These energies can be expressed in term values leading in a potential level diagram, as shown in Fig. 1.

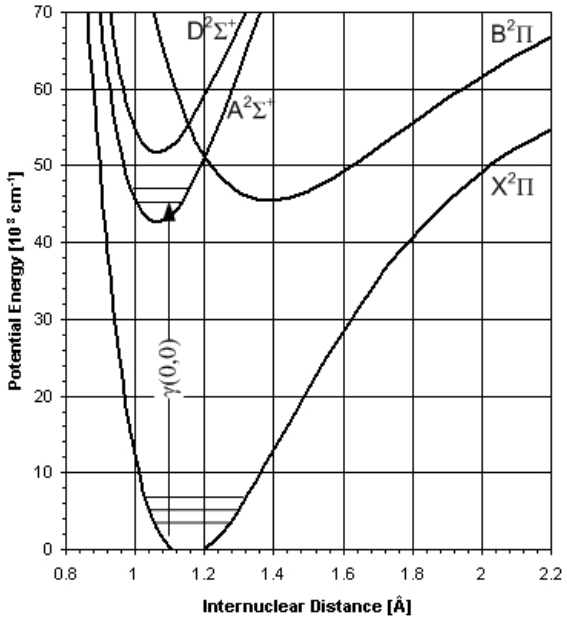

Fig. 1: Potential energy curves for nitric oxide

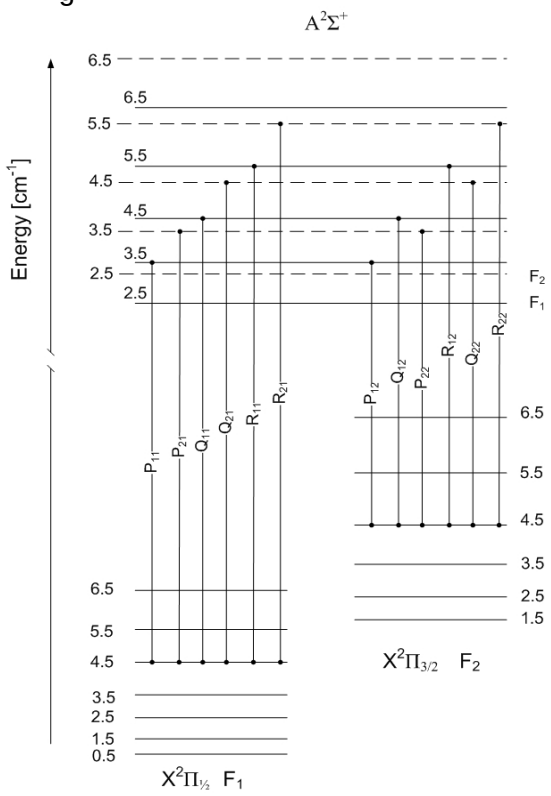

Fig. 2: Selection rules for transitions and the P, Q, R-branches

Selection rules

Only transitions between the ground level and the excited level that meet rotational selection rules are allowed. Possible transitions allow the change in the rotational quantum number ΔJ = -1, 0, +1, which is represented with the letters P, Q or R, respectively. The latin letters are followed by the subscript F'F'' indicating the total angular momentum quantum number Ω = 1/2 or 3/2.
The Λ-doubling describes the coupling between the rotational and electronic motion and leads to a splitting of each rotational level with the total angular momentum quantum number J to two closely spaced states with different parity. For spectroscopic notation the designation for the two components $(-1)^{J-1/2}$ and $(-1)^{J+1/2}$ is introduced, which are labelled as e and f, respectively (Geuzbroeck et al. 1991). However, the Λ-splitting is too small to be spectrally resolved by measurements. In Fig. 2 the relevant transitions between the different total angular momentum J of the lower state $X^2\Pi$ and the electronic higher state $A^2\Sigma$ can be seen. The splitting of the upper level designated by F_1 and F_2 is herby indicated by the dashed and solid line.
A further restriction is defined in ΔS = 0, thus only states with the same multiplicity are allowed, like $^2\Sigma \leftrightarrow {}^2\Sigma$, $^2\Sigma \leftrightarrow {}^2\Pi$, $^2\Pi \leftrightarrow {}^2\Pi$.
A common denomination concerning the electronic transitions between A ↔ X, B ↔ X and D ↔ X is given in the small greek letters γ, β, and ε, respectively. The change in the vibrational quantum number is attached to the greek letters; e.g. γ(v',v'') where v' and v'' refers to the upper and lower vibrational quantum number.

Excitation of molecules to higher states requires the selection of vibrational and rotational levels, which are highly populated in the ground state.

Equation (1) implies a distribution of the molecules given by the Boltzmann expression, where the level degeneracy (2J+1) and the partition function Q_{rot} must be accounted for.

$$\frac{N_J}{N} = \frac{(2J+1)}{Q_{rot}} e^{-E_{rot}/(kT_{rot})} \qquad (1)$$

The population of the rotational levels change with the rotational temperature, as can be seen in Fig. 3. For the selection of suitable excitation wavelengths, highly populated rotational levels, sufficient laser energy, and high Einstein coefficients for absorption (B_{12}) have to be considered. A simulation tool (Bessler 2003) of absorption and emission spectra assists to decide whether a transition is worth to be selected or not.

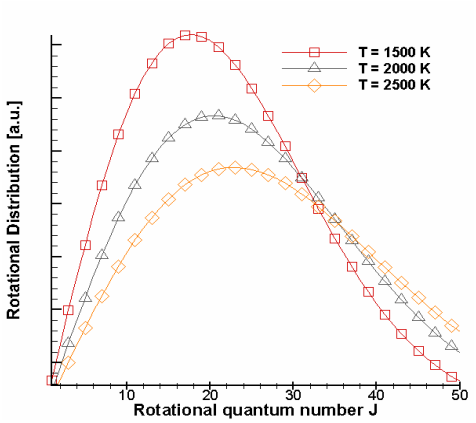

Fig. 3: Rotational distribution of the NO $X^2\Pi_{1/2}$ state as a function of rotational temperature

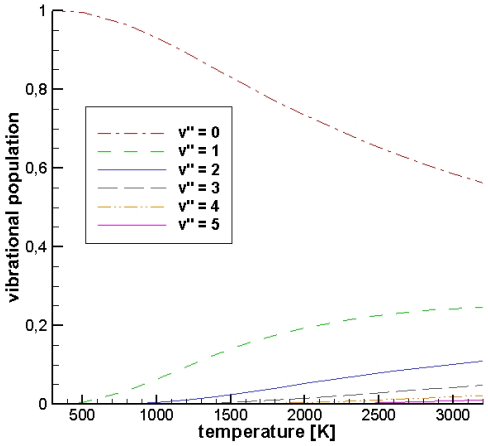

Fig. 4: Vibrational population fraction of the NO $X^2\Pi_{1/2}$ state as a function of vibrational temperature

The large tuning range of a dye laser enables the excitation of rotational quantum numbers up to J = 30, nevertheless in the case of a high enthalpy flow the strongest population is within the range of J = 12 - 22.
As shown in Fig. 4 only the v´´ = 0 vibrational state is sufficiently populated at temperatures below 500 K and quantification of NO by excitation in the A-X(0,0) band has been successfully executed (Bessler 2003).

Two level energy model

The fluorescence signal can be described by more or less complex models. Considering a molecular system where rotational relaxation is either frozen or completely equilibrated, the two level energy model would be appropriate (Herzberg 1950). The LIF principle consists of exciting a molecule from the lower level to the upper level, described as excited state. Each level can either be populated or depopulated by optical and collisional processes, which is mainly described by the rate constants b_{12} and b_{21}. These rate constants are related to the incident laser irradiance I_{Laser} and to the Einstein B coefficients B ($b = B/c\ I_{Laser}$), whereas the spontaneous emission is described through the Einstein coefficient A_{21}. Further processes like collisional quenching and photoionization are represented through the rate constants Q_{12} and W_{21}, respectively. In the case of an open two level model the loss of population from the upper level to a predissociative level is represented through Q_{diss}.
Photoionization and predissiociation are often negligible for excited states, unless specifically taken into account. In order to achieve a linear relation between the laser energy and the fluorescence signal, a certain level of the laser irradiance must not be exceeded. The upper level population can hereby be described through the rate constants, where steady state conditions can be reached. Hence, the fluorescence signal is proportional to the state popu-

lation density N and the Einstein coefficient A_{21} for spontaneous emission, and therefore a fluorescence transition rate is given by the product N_2A_{21}.
Relation (2) shows the dependency of the NO LIF intensity using the species density before laser excitation.

$$I_{\mathrm{LIF}} \propto I_{\mathrm{Laser}} N_{\mathrm{NO}} f_{\mathrm{B}} B_{12} g_{\lambda}(p,T) \frac{A_{21}}{A_{21}+Q_{21}} \tag{2}$$

At high laser excitation I_{Laser} the fluorescence signal I_{LIF} is exceeding the linear range and is mainly influenced by the number density N_{NO} of the excitable molecules times the Boltzmann fraction f_B. A dependency of the laser intensity and the collisional quenching rate Q no longer exists. Writing rate equations for the temporal derivatives of the rate population, the Einstein B coefficient for absorption, the spectral overlap $g_\lambda(p,T)$ of the laser profile and the fluorescence quantum yield $q_F = A_{21}/(A_{21}+Q_{21})$, have to be taken into account. The latter also known as fluorescence efficiency describes processes reducing the fluorescence signal. Since the collisional quenching rate is vital for quantitative measurements, one needs to know which are the quenching species and the temperature distribution within the system. If two different or more rotational states are probed, for instance in the field of multi-line thermometry and the ratio of the fluorescence signal is taken, the above mentioned dependencies cancels out and only a temperature variation can be observed.

In the case of a LIF experiment and during image acquisition with ICCD cameras, the LIF signal is recorded as camera signal S_f. Due to the lens system of the camera, the detection solid angle is defined as $\Omega/4\pi$ and η the detection sensitivity (combining filter losses, quantum efficiency, etc.). The measurement volume V is mainly determined by the laser sheet dimensions and therefore the solution for a two level model is:

$$S_f = I_{LIF} \frac{h\nu}{c} \frac{\Omega}{4\pi} V \eta \tag{3}$$

In the equation above the total fluorescence transitions are multiplied by the energy per photon, where h is Planck's constant, v is the frequency of the fluorescence and c the speed of light.

Experimental setup

The special design of the Y-shaped annular electrodes within the plasma torch offers long-duration testing, which is basically limited due to the amount of test gas. The gas in between the electrodes is ionised, becomes electrically conductive and a plasma is created. As the electrons leave the cathode, the electric field between the cathode and anode accelerates them, whereby thermal energy is transferred through collisions with heavy species. In the stagnation chamber, a stagnation temperature in the order of 6000 K is achieved. After passing a settling chamber where additional gas can be supplied, cooling the flow and hence covering a wider enthalpy range, the test gas is accelerated by expansion in a Laval nozzle. To achieve a broad spectrum of Mach numbers in the sub- or supersonic region, different nozzle contours are used.

Laser light from a Nd:YAG (Quanta Ray Pro 290, 550 mJ, 355 nm is achieved by mixing the fundamental and its second harmonic, repetition rate 10 Hz) pumped dye laser (Radiant Dyes, Coumarin 47, frequency doubled by a BBO) is used for the excitation of the NO molecule. Each image obtained is corrected for the laser energy, whereby the pulse energy measurement of the dye laser has been conducted using a pyroelectric element (Coherent, Energy Max Sensor 10-MB-HE). The sensor head is positioned behind a mirror to collect a fraction of the laser sheet energy.
To minimize thickness variations across the flow field a sheet-thining lens with a focal length of f = 500 mm (UV-antireflex coating) has been used. To avoid saturation effects a cylindrical

lens with f = - 45 mm was used to extend the laser beam. The ensuing fluorescence signal is collected perpendicular to axis of the laser beam and focused with a f/4.5 UV Nikkor lens onto a cooled intensified CCD camera (Andor Gen 2 A-DH334T-18F-E3).
Synchronization of the laser pulse and the micro channel plate (MCP) of the camera as well as the pyroelectric element is performed with the internal delay generator of the camera. Usually the gate width of the MCP is chosen in a way that it complies with the lifetime of the $A^2\Sigma^+$, v' = 0 state, which is 220 ns (Mcdermid et al. 1982), but due to quenching effects the lifetime will be rapidly reduced, hence the gate width was set to 70 ns.
A special NO-containing test cell was designed, which provides optical access to the gas via four fused silica windows as well as temperature and pressure instrumentation. The schematic of the experimental set up is shown in Fig. 4. The LIF system of this experiment is the same for both high enthalpy flow (Fig. 5) and preliminary measurements in a test cell.

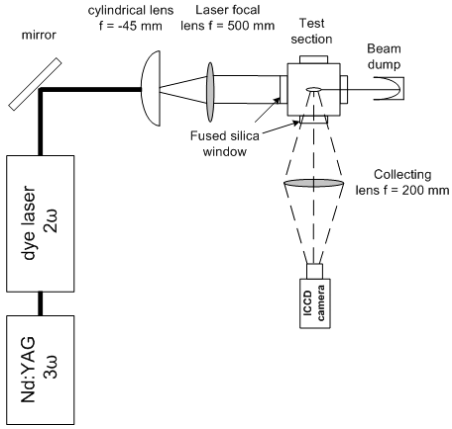

Fig. 4: Experimental setup for measurement of NO in a test chamber

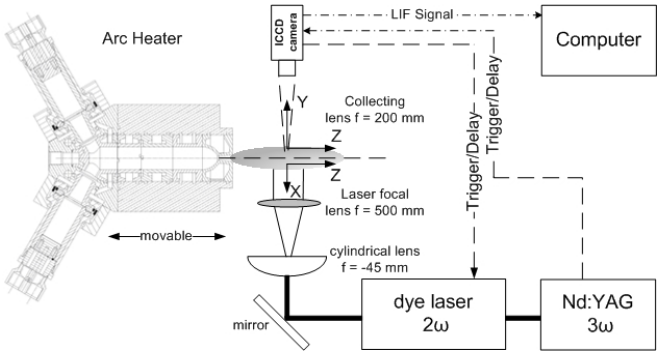

Fig. 5: Experimental measurement system of NO-LIF in an arc-heated plasma windtunnel

The first measurement principle requires an excitation scan, where the tuning range of the dye laser is scanned through the absorption lines of the NO molecule. The resolution is thereby given through the minimum wavelength increment of the dye laser, here 1 pm. The fluorescence is acquired over the full sensitivity range of the ICCD camera and recorded as a function of the excitation wavelength.

The second measurement principle is an excitation of fixed wavelengths with high absorption coefficients B_{12} of the NO molecule and thus leading to strong LIF signals, for instance only the Q_{22}-branch. To distinguish and extract specific lines within the excitation spectrum, the term energies of the excited and ground state have been calculated. Taking account of the transition rules, the wavelengths of the P, Q, R-branches can be calculated.
To proof the technical feasibility and the accuracy of the simulated spectra, a NO-containing test cell was designed and constructed. The cell can be heated up to 70°C, with the aid of a heating element mounted to the test cell. The high temperatures of the free stream are estimated to be 1000 K and 4000 K leading to a NO number density in the range of $1 \cdot 10^{16}$ cm^{-3} to $20 \cdot 10^{16}$ cm^{-3}, predicted by a chemical equilibrium calculation. In order to met those condition a mixture of NO and N_2 (1650 ppm NO, Messer-Griesheim, Cologne, Germany) has been used.

Results and Discussions

Previous studies have shown that variation in fluorescence quantum yield and variation in spectral overlap with the laser profile arises from line broadening (DiRosa et al. 1994). LIF interferences due to other species are mainly affected by the appropriate selection of a single rotational line for absorption feature. In practice, however, it is almost impossible to pump a single absorption transition and thus a single ro–vibrational state. Taking these restrictions into account an excitation scan is recorded to increase the signal strength. The excitation-

emission chart presented here is acquired by tuning the laser by several wavenumbers within the γ(0,0) band and fluorescence is collected using a broadband detection, typically the γ(0,1) band is used since its Franck-Condon factor is the largest.
An optimized strategy for NO detection should involve separation of background noise and fluorescence signal yielding in maximum signal-to-noise ratio. Radiation emitted by the high enthalpy flow is a major cause for interferences, thus the fluorescence signal is corrected by a background image without laser illumination.

For comparison and validation of the calculated excitation spectra, preceding measurements at room temperature have been carried out using a test cell filled with nitric oxide (Fig. 6 and 7). Consequently, five laser shots were accumulated, to take into account shot to shot variations of the dye laser energy.

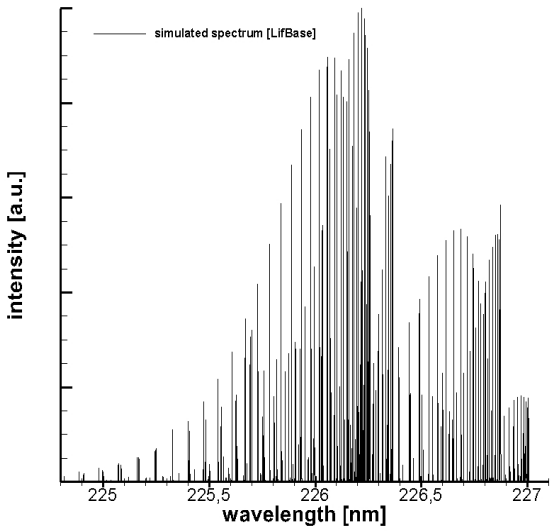

Fig. 6: Simulated excitation scan at T = 290K (Bessler et al. 2003)

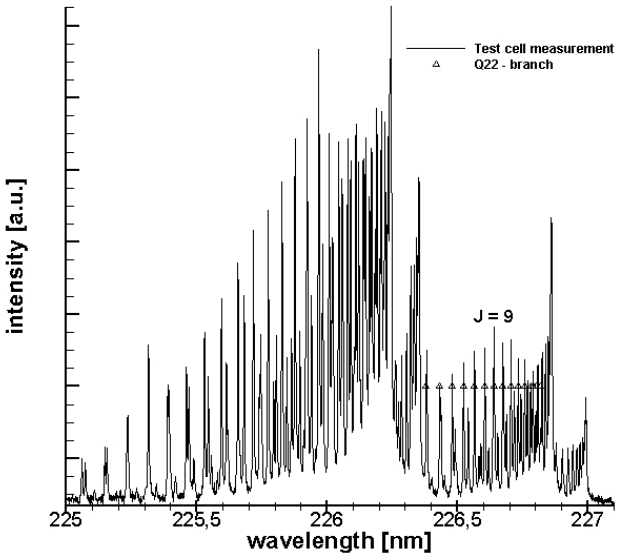

Fig. 7: Measured excitation scan at T = 290 K and the line positions of the Q_{22}-branch up to J = 20

Laser induced measurements of nitric oxide in high enthalpy flows requires a total enthalpy of less than 10 MJ/kg, otherwise no fluorescence is observable (Mizuno et al. 2007). Equilibrium calculations show, that the NO mole fraction decreases with increasing temperature above 3000 K. Hence, an operational condition with a total enthalpy of 3 MJ/kg and a total gas mass flow of 14 g/s was chosen.

The spatial distribution of nitric oxide of the flow field behind the nozzle exit at the distance of 20 mm is shown in Fig. 8, excluding the intensity distribution of the laser sheet and the beam attenuation due to absorption of nitric oxide. The beam attenuation is dependent on the NO concentration in the flow field and is assumed to stay constant during image acquisition. However, one can see strong fluorescence intensity values at the shear layer, and lower values in the core region, which results from the lower temperature values in the outer region, which leads to increased combination of dissociated oxygen and nitrogen.
A measured excitation spectrum is extracted from the shear layer by averaging a small uniform 10 x 10 pixel area and shown in Fig. 9. Some transitions have been identified so far; especially in the wavelength range above 226.3 nm the Q_{22}- and the O_{12}-branch are clearly visible. For a better validation of the spectrum a small wavelength range is zoomed out and superimposed with the calculated positions of the Q_{22}-branch, which are indicated in small squares. A further consideration includes a selection of spectrally isolated lines to determine the rotational temperature through a Boltzmann-plot.

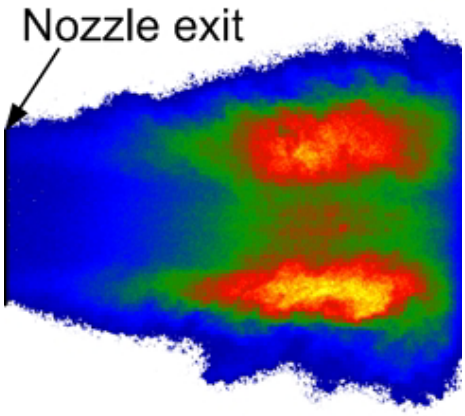

Fig. 8: Qualitative PLIF image of nitric oxide in high enthalpy flow. The laser sheet is passing from the bottom to the top

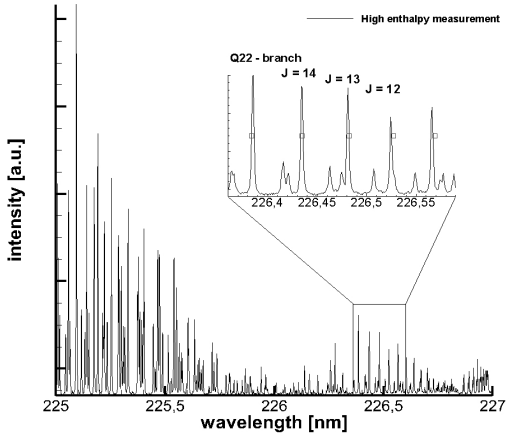

Fig. 9: Measured excitation scan in a high enthalpy flow and the line positions of the Q_{22}-branch

Conclusions and Outlook

Laser induced fluorescence of nitric oxide in a high enthalpy flow was observed for a total enthalpy of 3 MJ/kg. In addition an excitation scan in a test cell, as well as in a high enthalpy flow, has been successfully performed.
The accuracy of the evaluated transitions has been confirmed using a comparison of the calculated results with the measured spectrum. The measured excitation scan show excellent agreement with the simulated spectrum at room temperature. Measurements performed in a high enthalpy flow provide information about suitable transitions to derive the rotational temperature.
In order to calculate the rotational temperature of nitric oxide, appropriate transitions like the Q_{22}-branch have been selected. To achieve a more accurate temperature measurement, the effects of beam attenuation due absorption and transition saturation have to be considered.
It is planned to conduct further measurements to determine the rotational temperature of nitric oxide in a high enthalpy flow.

Refereneces

Bessler W. G., Schulz C. et. al., 2003: “Strategies for laser-induced fluorescence detection of nitric oxide in high-pressure flames”, Applied optics, Vol. 42, No. 12
Bessler W. G., Schulz C., Sick W. G., Daily J. W., 2003: “LIFSim, A versatile modeling tool for NO and O_2 LIF spectra”. http://www.pci.uni-heidelberg.de/pci/lifsim/
DiRosa, M. D. and Hanson, R. K., 1994: “Collisonal-broadening and shift of NO (0,0) absorption lines by O_2 and H_20 at high temperatures”, J. Quant. Spectrosc. Radiat. Transfer 52, 515-529
Geuzebroeck F. H., Tenner M.G., Kleyn A.W., Zacharias H., S. Stolte, 1991: “Parity assignment of Λ-doublets in NO $X^2\Pi_{1/2}$”, Chemical Physical Letters, Vol. 187, No. 4, pp 520-526
Hatzl S., Sander T., Mundt Ch., 2011: “One-Dimensional Measurements of High Enthalpy Flow Temperature Using Spontaneous Raman Spectroscopy”, 17th International Space Planes and Hypersonic Systems and Technologies Conference, San Francisco
Herzberg G., 1950: “Molecular Spectra and Molecular Structure I. Diatomic Molecules”, (D. Van Nostrand, Princeton, NJ)
Hollas J. M., 1995: „Moderne Methoden in der Spektroskopie“, Vieweg, Braunschweig, 202-241
Langkau, R. U. 1981: „Eine neue Forschungsanlage zur Untersuchung chemischer Reaktionen in Gasströmungen hoher Enthalpie“, Dissertation, Universität der Bundeswehr München
Mcdermid S. and Laudenslager J. B., 1982: “Radiative lifetimes and electronic quenching rate constants for single-photon-excited rotational levels of NO ($A^2\Sigma^+$, v = 0)”, J. Quant. Spectrosc. Radiat. Transfer, Vol. 27, No. 5, pp. 483-492
Mizuno M., Ito T., Ishida K., Nagai J., 2007: “Laser induced fluorescence of nitric oxide and atomic oxygen in an arc heated wind tunnel”, 39th AIAA Thermophysics Conference, Miami FL, 25 -28
Yamada T., Inatani Y., 2002: “Nonequilibrium Temperatures Measurement in an Arc-Heated Airflow by the Optical Diagnostic Method”, Trans. Japan Soc. Aero. Space Sci., Vol. 45, No. 148, pp 83-93